PHYSICAL REVIEW B VOLUME 44, NUMBER 17 1 NOVEMBER 1991-I

Structural, electronic, and magnetic properties of rare-earth metal surfaces: hcp Gd(0001)

Ruqian Wu, Chun Li, and A. J. Freeman
Department of Physics and Astronomy, Northwestern University, Evanston, Illinois 60208-3112

C. L. Fu
Oak Ridge National Laboratory, P.O. Box 2008, Oak Ridge, Tennessee 37831
(Received 14 March 1991)

Structural, electronic, and magnetic properties of the hcp Gd(0001) surface have been determined using the all-electron local-density full-potential linearized augmented-plane-wave method. A precise total-energy analysis reveals that (1) surface Gd atoms occupy the hcp sites; the outermost interlayer spacing expands by $\sim 6\%$; (2) the surface Gd layer couples antiferromagnetically with the underlying ferromagnetic bulk; and (3) the energy stability of the surface antiferromagnetic coupling arises from the enhancement of the second-neighbor interactions. A localized d_{z^2} surface state is found near the $\bar{\Gamma}$ point, which is occupied (empty) in the majority (minority)-spin band and results in an enhancement of the surface magnetic moment.

I. INTRODUCTION

Of the rare-earth (RE) metal surfaces, Gd(0001) has attracted considerable attention in recent years because of its interesting magnetic properties. Pioneering work by Rau *et al.*[1] using electron-capture spectroscopy and by Cerri, Mauri, and Landolt[2] using spin-polarized photoemission, reported the existence of surface ferromagnetic (FM) order at temperatures up to 310 K ($\sim$20 K above its bulk Curie temperature $T_{C,b}=293$ K) on polycrystalline Gd thin films. Weller *et al.*,[3] employing spin-polarized low-energy electron-diffraction (SPLEED) and magneto-optic Kerr-effect (MOKE) techniques, confirmed this so-called surface-enhanced magnetic-order (SEMO) phenomenon on epitaxial hcp Gd(0001) thin films grown on a single-crystal W(110) substrate and, furthermore, interpreted their results to indicate an antiferromagnetic (AFM) coupling between the surface $4f$ spins and those of the underlying FM bulk. They later claimed[4] that the SEMO is strongly dependent on the presence of an external magnetic field during cooling across the $T_{C,b}$ and connected it to a surface first-order phase transition.[5] Farle and Baberschke[6] reported that the Curie temperature depends on the film thickness [grown on a W(110) substrate]; the T_C of a Gd monolayer on W(110) is 20 K below $T_{C,b}$.

Concerning the ground-state properties, Himpsel and Reihl[7] measured the $6s$,$5d$ bands and work function for Gd(0001). LaGraffe, Dowben, and Onellion[8] observed (i) FM ordering in ultrathin Gd films on Cu(100) substrates using synchrotron-radiation photoemission, (ii) an exchange splitting that changes from approximately 1.1 to 0.6 eV as the overlayer thickness increases from one to six layers, and (iii) the binding energy of the Gd $5d$- and $4f$-electron states are 0.3–0.4 and 8.0–8.6 eV, respectively. In their other work,[9] the surface-to-bulk $4f$ core-level shift for Gd thin films on Cu(100) was found to be 0.3–0.4 eV. By comparison, a $4f$ core-level shift of 0.48 eV for the clean Gd surface was measured by Kammerer *et al.*[10] with synchrotron-radiation-excited photoemission. Structural properties of Gd thin films on a W(110) substrate were also studied by Kolaczkiewicz and Bauer[11] with Auger electron spectroscopy (AES), low-energy electron diffraction (LEED), TDS, and work-function measurements.

The magnetic coupling between Gd films and $3d$ transition metal or other rare-earth (RE) metals is also important because of the application as permanent magnets and high-density storage media.[12] In alloys and compounds, Gd spins are found to align antiparallel to that of transition-metal $3d$ electrons.[13] This antiparallel alignment was found in a carefully prepared Gd/Fe(001) interface.[14–16] Kwo *et al.*[17] also reported possible AFM Gd-Gd coupling and lower magnetic moments across the interfacial region in the Gd/Y superlattice.

As a prototype of a RE metal, the electronic and magnetic properties of hcp bulk Gd have been explored extensively by means of band-structure calculations.[18] In both gas and solid phases, Gd has a stable trivalent $4f^7(5d6s)^3$ configuration. The half-filled $4f$ shell carries zero total orbital angular momentum and a maximum spin, i.e., $L=0$, $S=\frac{7}{2}$, $J=\frac{7}{2}$, and $g=2.0$. Pioneering theoretical work[19–21] pointed out that the indirect exchange via $5d$ conduction electrons is the dominant factor to determine the magnetic alignment of $4f$ spins. The average exchange splitting of the $5d$-electron bands is $\sim$0.6 eV, and the magnetic moment from conduction electrons, M_v, is $\sim 0.7\mu_B$.[19] By including the spin-orbit Hamiltonian as a perturbation, Sticht and Kübler[22] calculated the M_v to be $0.64\mu_B$. Recently, a linear muffin-tin orbital (LMTO) calculation of the rare-earth ground- and excited-state properties reported by Min *et al.*[23] found M_v to be $0.70\mu_B$. Finally, the electronic and magnetic properties of bcc-ordered Gd metal were also determined by Leung, Wang, and Harmon;[24] their linear augmented-plane-wave (LAPW) calculations yielded a

M_v of $0.75\mu_B$/atom.

For Gd(0001) and other rare-earth metal surfaces, the theoretical understanding of the ground state and critical properties lags far behind the accumulated experimental determinations. Monte Carlo studies based on the Ising model revealed that the SEMO (Ref. 25) may occur only when the ratio of the surface exchange J_s and bulk exchange J_b, (i.e.), J_s/J_b, becomes larger than a critical value ~ 1.52. Thus the exchange interaction in the Gd(0001) surface layer must be greatly enhanced in order to realize the SEMO. In a recent full-potential linearized augmented-plane-wave (FLAPW) energy -band investigation, we reported that the M_v of a free-standing hcp, ferromagnetic Gd monolayer is about $0.8\mu_B$ inside the muffin-tin spheres ($1.0\mu_B$/atom if the contribution in other regions is included).[26] Compared to the corresponding hcp bulk Gd result of $\sim 0.46\mu_B$ ($\sim 0.58\mu_B$/atom in the whole space), this moment is enhanced by about 70%, because of the reduced coordination number.

In this paper we report FLAPW results of the structural, electronic, and magnetic properties for the hcp Gd(0001) surface. Accurate total-energy results show that the surface Gd atomic layer expands outwardly by $\sim 6\%$. The AFM surface coupling is the ground state—which supports the experimental interpretation by Weller *et al.*[3] In the following we describe briefly the methodology and computational model in Sec. II. Results and discussions of the total energy, charge density, and work function, spin density, magnetic moments, hyperfine field, band structure, exchange splitting, and surface $4f$ core-level shift, etc., are presented in Sec. III. In Sect. IV we give a brief summary and conclusion.

II. METHODOLOGY AND COMPUTATIONAL MODEL

The FM and AFM Gd(0001) surfaces, as shown in Fig. 1, are simulated primarily by an hcp slab geometry with six Gd atomic layers. This choice is reasonable since test calculations carried out on an eight-layer AFM slab confirm most of the results. The two-dimensional 2D lattice constant and distances between adjacent bulk layers were taken from experiment ($a = 6.8446$ a.u., $c = 10.8622$ a.u., and $c/a = 1.587$), while the distance between the surface and underlying bulk layers is determined by minimizing the total energy. To determine possible fcc stacking at the surface, we also investigated the case in which the surface Gd atoms are located on fcc sites.

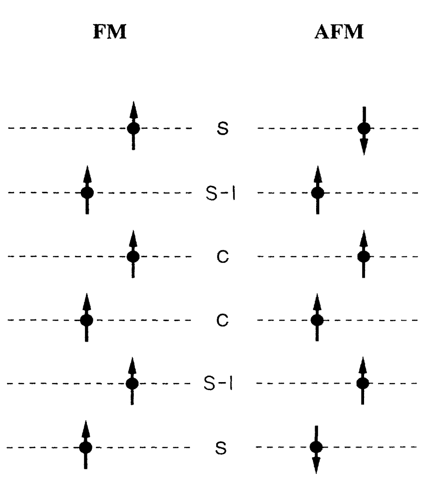

FIG. 1. Schematic ferromagnetic and antiferromagnetic configurations for a six-layer Gd(0001) slab.

The Kohn-Sham LDF equations are solved self-consistently by means of the all-electron full-potential linearized augmented-plane-wave method[27]— which is free from any shape approximations to the charge densities, potentials and matrix elements. The core states are treated fully relativistically and the valence states are treated semirelativistically (i.e., without spin-orbit coupling).[21] We employ von Barth and Hedin's formula for the exchange-correlation potential.[28] Although the local-density approximation has some inherent deficiencies [e.g., predicting a few percent smaller lattice constant and failing to obtain the correct magnetic ground state for bulk Fe (Ref. 30)], this approach has been applied very successfully in the last decade to determine the structural, electronic, and magnetic properties of many transition-metal systems.[29] For rare-earth metals the LDF band description cannot be used for the $4f$ electrons because of their strongly localized character. Thus their description as core electron states, as is done here, is appropriate. Further, since the majority spin $4f$ level lies far below (6–8 eV) the Fermi energy and the $4f$ electrons only occupy a small region around the nucleus ($\bar{r} = 0.85$ a.u.), the calculated results for the conduction-band states should have the same validity as that obtained for transition-metal systems.[29]

About 90 augmented plane waves per Gd atom are used as a variational basis set. Within the nearly touching muffin-tin (MT) spheres ($r_{\rm MT} = 3.35$ a.u.), lattice harmonics with angular momentum l up to 8 are employed to expand the charge density, potential, and wave functions. As was done previously for Gd metal, the $4f$ electrons are treated as core electrons with the majority spins fully occupied and minority spins empty. This means that intersite $4f$ and on-site $4f$-$5d$ hybridizations are neglected. The **k**-space integrations are substituted by direct summations over 21 well-distributed **k** points in $\frac{1}{12}$ of the irreducible 3D Brillouin zone BZ. Convergence is assumed when the average mean-squared distance between the input and output charge densities is less than $5\times 10^{-4} e/(a.u.)^3$, making the total-energy results reliable to 1 mRy.

III. COMPUTATIONAL RESULTS

A. Total energy

To determine the equilibrium surface atomic and magnetic structure, we plotted the calculated total energy as a function of the surface interlayer distance, $d_{s,s-1}$, in Fig. 2 for Gd(0001). The solid circles and solid rhombi represent the results for the FM and AFM phases, re-

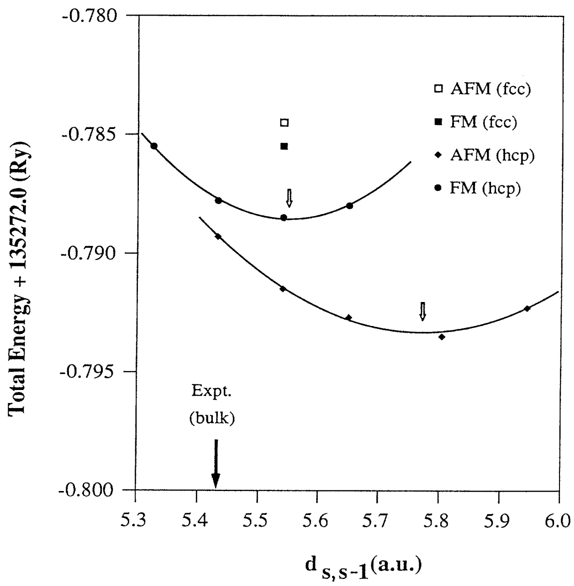

FIG. 2. Theoretical total energy of the Gd(0001) surface vs the distance between the surface (s) and adjacent underlayer ($s-1$). The circles (for FM) and rhombi (for AFM) represent the results for hcp stacking, while the squares (solid for FM, open for AFM) represent the results of the film with surface fcc stacking. The open arrows show the equilibrium positions obtained by total-energy minimization. The solid arrow points out the experimental distance.

spectively. Obviously, the theoretical data can be well fitted by a parabola (solid lines). The minimum in each fitted curve, pointed out by the arrows, gives the calculated equilibrium distance $d_{s,s-1}=5.55$ a.u. for the FM case and $d_{s,s-1}=5.77$ a.u. for the AFM case. Compared to the experimental interlayer distance in hcp Gd bulk ($c/2=5.43$ a.u.), the surface interlayer spacing of Gd(0001) *expands* by about 6.3% and 2.2% for AFM, and FM configurations respectively.

Generally, surface relaxation is driven by several factors: (1) rehybridization with the underlying layers to saturate the dangling bond, (2) minimization of the kinetic and exchange-correlation energy of the interstitial electrons, and (3) enhancement of surface magnetic polarization. Among these, the first factor tends to shrink the interlayer distance so as to gain bonding energy. The kinetic and exchange-correlation energy, based on the LDA formula,[28] favors a larger interatomic spacing for most of metals ($r_s \leq 4.0$ a.u.). The magnetic pressure, as reported for Fe, Co, Ni, Cr, and Mn bulk crystals[31] and, recently, an overlayer system Fe/Ru(0001),[32] also expands the lattice. The equilibrium relaxation is determined by neutralizing these competing forces.

Compared to transition metals, which usually show a 3–7% surface compression,[33] the rare-earth metals have much more extensive $5d$ and $6s$ wave functions and a lower valence occupation—which results in softness of the lattice (cf. the small modulus of Gd metal[34]). Consequently, the first factor is weaker for Gd. Meanwhile, the giant $4f$ magnetic moment induces positive magnetic (spin-density) polarization in the whole space. Larger interatomic distances, with only a little cost in the binding energy, is, of course, favorable for providing more volume for the magnetic polarization and, furthermore, for easing the kinetic-energy cost.

For the AFM case, the majority spin surface states couple with the minority spin states of the underlying bulk. The surface interlayer interaction is even weaker than that for the FM case. Moreover, the expanded surface interlayer spacing can enhance magnetic polarization in both the surface and second layers. Therefore, AFM coupled surface layer expands even more compared to the FM case.

Significantly, the calculated minimum of the total energy for AFM coupling is about 5 mRy lower than that for FM coupling. The surface AFM coupling is the ground state for Gd(0001)—which supports experimental interpretation of Weller *et al.*[3] However, since the FM coupling may also exist under certain conditions (e.g., high magnetic field, etc.) as a metastable state, we will discuss both FM and AFM phases together hereafter.

For the surface fcc-stacked case, we found that the surface layer also expands outwardly.[35] At a chosen surface interlayer spacing of 5.55 a.u. [corresponding to the equilibrium spacing for hcp FM Gd(0001)], the calculated total energies are shown by squares in Fig. 2. Obviously, they lie far above (3–7 mRy) the total energies of the corresponding hcp geometry and so surface fcc stacking is not energetically favorable. Note that the total energies for the FM and AFM change their ordering now compared to that for hcp stacking. We may therefore infer that since the nearest-neighbor configurations around the surface atoms are the same for these two kinds of stacking, the surface magnetic ordering appears to be determined by details of the second-nearest-neighbor interactions.

B. Valence charge density and work function

The total valence charge densities on the $(11\bar{2}0)$ plane are presented in Fig. 3(a) and 3(b) for the FM and AFM hcp Gd(0001) surfaces, respectively. From these contour plots, we see that the electrons in the surface atoms spill out into the vacuum region to lower their kinetic energy. The density corrugation along the horizontal direction is very small, even not far above the surface atoms, indicating the smoothness of the Gd(0001) surface. It is striking that the spatial charge distribution just below the surface layer shows a typical metallic interaction between the Gd atoms without noticeable special bond orientation.

The spatial distribution of the difference between the AFM and FM valence charge densities shown in Fig. 3(c) (with $d_{s,s-1}=5.55$ a.u.) provides a physical picture with which to understand the energy stability of the surface AFM coupling. Obviously, the bonding between the surface and center layer seen in the figure indicates that the surface AFM stability originates from the enhancement of the second-neighbor interaction—in support of the inference from the total-energy analysis given earlier.

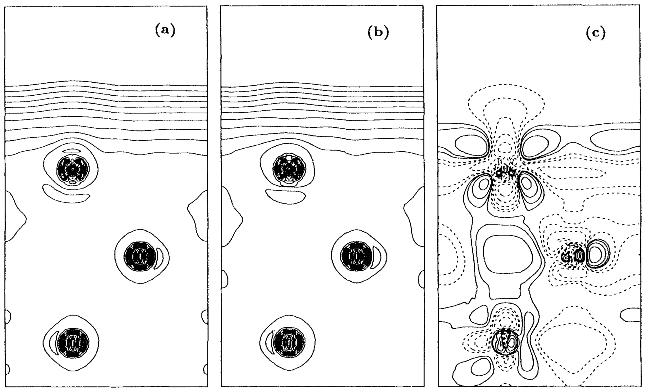

FIG. 3. Total valence charge density of (a) FM Gd(0001), (b) AFM Gd(0001), and (c) their difference ($\rho_{AFM}-\rho_{FM}$) on the vertical $(11\bar{2}0)$ plane. Contours in panels (a) and (b) start from 5×10^{-4} and increase successively by a factor of $\sqrt{2}$. Contours in panels (c) start from $\pm1.0\times10^{-4}$ and increase successively by a factor of 2.

In Table I the total and l decomposed charge in each muffin-tin sphere and the charge in the interstitial and vacuum regions are listed for majority and minority spins, together with the corresponding results for FM Gd bulk (denoted by B). From these data we find that (1) the different surface magnetic ordering barely influences the integrated number of electrons in each region, even in the surface MT sphere; (2) the total and l decomposed charges inside the center layer (C) MT spheres obtained from the FM and AFM six-layer slab calculations are almost identical to the corresponding result for FM Gd bulk—suggesting that the six-layer slab is reasonably thick enough; (3) electrons in the MT spheres are predominantly d like, although the average valence charge density in these regions [about $0.0140e/(\text{a.u.})^3$] is almost equal to that in the interstitial region [$0.0136e/(\text{a.u.})^3$]; and (4) there are about 10% fewer electrons in the surface MT spheres than in the underlying spheres because of charge spilling out into the vacuum. As a result of the spillage, the $4f$ binding energy is enhanced at the surface by 0.35 eV for both the FM and AFM cases, in good agreement with the experimental results (0.3–0.4 eV).[9]

The calculated work functions of the AFM and FM Gd(0001) surfaces are 3.67 and 3.84 eV, respectively. These results are, however, larger than the corresponding experimental work function, 3.3 ± 0.10 eV,[7] and the work function obtained from a polycrystalline Gd film, 3.1 ± 0.15 eV.[36] This deviation is unlikely due to the insufficiency of the slab thickness since the work function obtained from an eight-layer AFM slab (3.70 eV) is very close to that obtained from the six-layer AFM slab. It most probably arises from the counterpolarization of surface semicore shells ($5s,5p$),[37] which is not included in present treatment.

C. Spin density and magnetic moments

Figure 4 presents the calculated valence spin densities on the $(11\bar{2}0)$ plane for the FM and AFM hcp Gd(0001)

TABLE I. Total and l decomposed charge (in electrons/unit cell) in each muffin-tin sphere (MT radius is 3.35 a.u.), in interstitial and vacuum regions, and the work functin (in eV) for AFM and FM hcp Gd(0001) surfaces.

		FM			AFM		
		Spin 1		Spin 2	Spin 1		Spin 2
B	s	0.248		0.238			
	p	0.207		0.125			
	d	0.867		0.488			
	total		2.192				
C	s	0.247		0.237	0.258		0.253
	p	0.206		0.131	0.207		0.131
	d	0.875		0.500	0.852		0.478
	total		2.207			2.200	
$(S-1)$	s	0.242		0.239	0.260		0.243
	p	0.209		0.128	0.201		0.147
	d	0.860		0.505	0.817		0.495
	total		2.180			2.181	
S	s	0.249		0.219	0.235		0.266
	p	0.147		0.092	0.094		0.140
	d	0.866		0.393	0.408		0.829
	total		1.986			1.988	
Inter.			4.961			4.972	
Vacuum			0.292			0.288	
Work function			3.84			3.67	

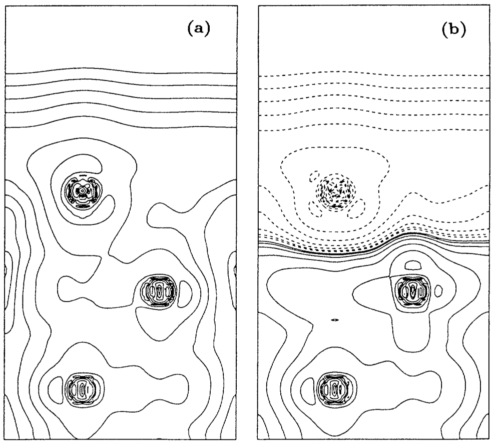

FIG. 4. Spin densities on the $(11\bar{2}0)$ plane for (a) Fm Gd(0001) and (b) AFM Gd(0001). Contours start from $\pm 1.0\times 10^{-4} e/(\mathrm{a.u.})^3$ and increase by a factor of 2.

surfaces. Because the valence spin polarization is induced by the $4f$ shell through direct exchange coupling, the majority spin exceeds the minority spin in the whole space for the FM surface—which is different from the usual results for transition metals. For the AFM case, since the $4f$ spin polarization in the surface layer is antiparallel to that of the underlying layers, the valence spin density in surface region becomes negative in order to follow this polarization.

The calculated M_v is listed in Table II. For FM Gd bulk, M_v in the muffin-tin sphere, $M_{v,\mathrm{MT}}$, is $0.47\mu_B$. Adding the contribution from the interstitial region, $M_{v,\mathrm{int}}=0.12\mu_B$, the total calculated $M_v=0.59\mu_B$/atom. This value agrees well with experimental result $(0.63\mu_B)$,[38] suggesting the validity of present day theoretical treatments. For the FM state, the conduction-electron magnetic moment in the surface muffin-tin sphere is enhanced by about 20%. It shows a slight Friedel oscillation approaching the center layer, and the moment in the center-layer muffin-tin sphere still differs a little from that in the bulk—indicating a possible size effect in this six-layer film. For the AFM state, the induced valence spin density decreases markedly (with a node in the in-between region) and the magnetic moments in the topmost two layers become smaller than those for the FM coupling. Nevertheless, the surface magnetic enhancement is noticeable because the negative surface magnetic moment is still larger than the corresponding value in the center-layer MT sphere.

TABLE II. Calculated magnetic moments for bulk Gd and the GD(0001) surface.

		FM	AFM
Gd bulk	MT	0.47	
	int./atom	0.12	
	total	0.59	
	expt.	0.63	
Gd(0001)	S	0.58	−0.49
	S-1	0.44	0.41
	C	0.46	0.45
	int./atom	0.14	

D. Fermi-contact hyperfine field

The magnetic hyperfine interaction, which describe the coupling of electronic spin to the nuclear magnetic moment, can be measured directly via the Mössbauer effect. The Fermi contact part of this hyperfine field, H_{CF}, is proportional to the electronic spin density at the nucleus and is usually divided into contributions from core and valence electrons. As a well-established fact for magnetic transition-metal bulk, surfaces, and overlayers, the core contribution is proportional to the local moment and is negative in sign.[39] The valence contribution, however, depends very sensitively on the environment.

The calculated hyperfine fields for FM and AFM Gd(0001) are presented in Table III, where the contribution of the core electrons is further decomposed into

TABLE III. Fermi-contact hyperfine field for FM hcp bulk Gd and the Gd(0001) surface (in kG).

	Gd bulk	FM			AFM		
		C	S-1	S	C	S-1	S
H_{CF}	−245	−239	−500	537	−373	296	−425
Valence	107	110	−175	1091	−15	606	−830
Core	−352	−349	−326	−554	−358	−309	405
$1s$	0	0	0	0	0	0	0
$2s$	−823	−823	−823	−828	−828	−823	828
$2p$	−27	−26	−26	−27	−26	−27	27
$3s$	−8709	−8712	−8708	−8717	−8741	−8742	8752
$3p$	−445	−445	−445	−445	−446	−446	447
$4s$	1041	1041	1039	1046	1044	1042	−1047
$4p$	57	57	57	57	57	57	−57
$5s$	8131	8137	8157	7949	8159	8202	−8121
$5p$	430	429	430	415	430	432	−426

different shells (only $j=\frac{1}{2}$, corresponding to $\kappa=1$ in the Dirac equation). Note that the negative core contribution results from the compensation between large contributions from inner shells (negative, predominantly 3s) and outer shells (positive, predominantly 5s). For the FM Gd bulk, the valence (5d,6s,6p) spin density is positive at the nucleus and partly offsets the negative core contribution. For FM Gd(0001) the valence contribution oscillates drastically in the outermost two layers when approaching the bulk. Nevertheless, the hyperfine field, both the valence and core parts, becomes identical to the corresponding bulk value at the center layer, suggesting the short-range screening effect on the magnetic properties. For the AFM surface, the core contribution at the surface changes to positive to follow the 4f polarization. The oscillation even penetrates to the center layer of the

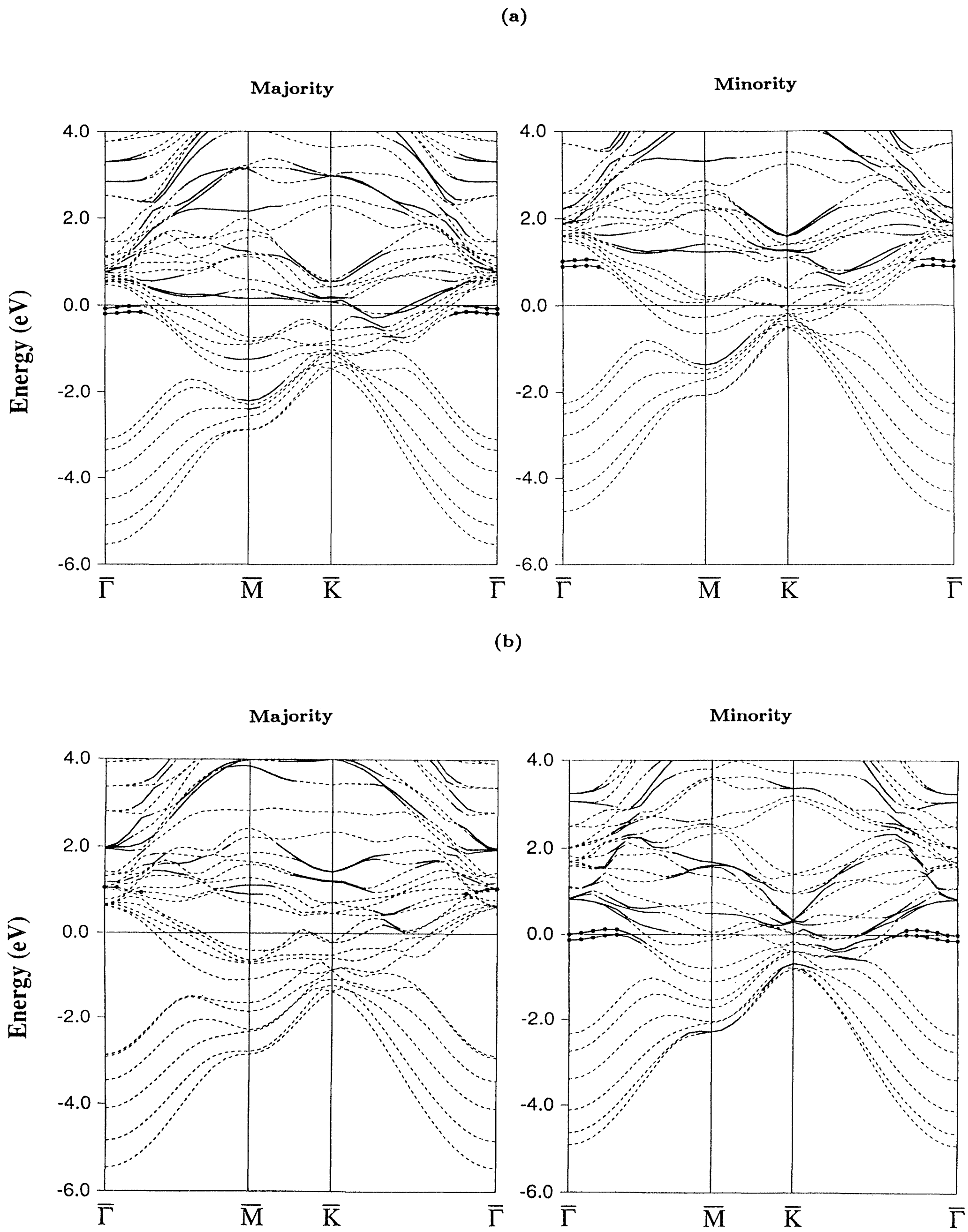

FIG. 5. Energy bands along the high-symmetry directions of (a) FM Gd(0001) and (b) AFM Gd(0001). Solid lines represent states with more than 50% weight in the surface muffin-tin sphere. Solid circles show the surface states with more than 70% projection in surface region.

six-layer slab. However, the hyperfine field at the center layer of the eight-layer slab converges to 247 kG. Thus the magnetic disturbance in Gd metal is likely limited to second neighbors.

Corresponding to the surface magnetic-moment enhancement, the core contribution is enhanced greatly at the surface layer. This enhancement, as shown in Table III, arises only because the positive contribution from 5*s* and 5*p* outer shells decreases. Although the core-hyperfine field $H_{\mathrm{CF},c}$ (in kG) does not show an explicit proportionality to either the total or conduction magnetic moment, it can be well fitted by a linear dependence

$$H_{\mathrm{CF},c} = 58M_{4f} - 1660M_{v,\mathrm{MT}} , \tag{1}$$

for Gd bulk and for FM and AFM Gd(0001). Therefore, the rule, that the core-hyperfine field is proportional to the local moment, still holds for this RE metal, but one must separate the influence of *f* electrons from that of the 5*d* conduction electrons. The 4*f* shell induces a positive contribution because it lies ($\bar{r}=0.85$ a.u.) well inside the 5*s*,5*p* core shells ($\bar{r}=1.32-1.60$ a.u.). The valence-induced part is negative and is very sensitive to the conduction electronic magnetic moment due to the large polarization per moment, 1660 kG/μ_B, which is about 10 times larger than the ratio obtained for transition metals, 140–150 kG/μ_B.[39]

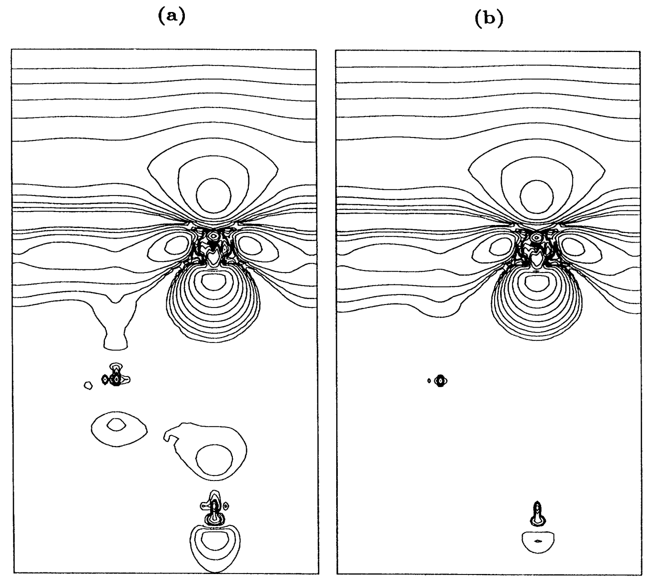

FIG. 6. Single-state charge density of the $\bar{\Gamma} d_{z^2}$ surface states just below the Fermi level on the (11$\bar{2}$0) plane for (a) FM Gd(0001) and (b) AFM Gd(0001). Contours start from $2.5\times10^{-4} e/(\mathrm{a.u.})^3$ and increase by a factor of $\sqrt{2}$.

E. Energy bands, density of states, and surface states

In order to delve more deeply into the physical origin of the magnetism of the Gd(0001) surface, we discuss the band structure and density of states. In Fig. 5 the bands along the high-symmetry directions in the 2D Brillouin zone are plotted for both the FM and AFM coupled Gd(0001) surfaces. The solid lines denote states with more than 50% weight in the surface muffin-tin sphere, while solid circles emphasize the surface states (SS) with larger surface and vacuum projection ($\geq 70\%$).

Significantly, there are two outstanding branches of a localized surface state (they should be degenerate if the slab is thick enough) lying in the bulk gap within $\frac{1}{3}-\frac{1}{4}$ of the way from the $\bar{\Gamma}$ point to the edge of the BZ for both AFM and FM coupling. For the FM case, they are occupied (0.1 eV below E_F) for majority spin, but are empty (1.2 eV above E_F) for minority spin. This difference in the occupation, however, is the most important physical origin of the surface magnetic-moment enhancement. For the AFM state, surface majority-spin bands interact with the interior minority-spin bands. The SS now appears in the minority bands and becomes half-filled (one of the branches). The occupation, i.e., the position of the SS with respect to the Fermi energy, is independent of the slab thickness as confirmed by eight-layer test calculations.[40] In the majority part (surface minority), the SS merges into the bulk bands and loses its localization very quickly away from the $\bar{\Gamma}$ point due to hybridization with the bulk states.

Obviously, as shown by the single-state charge-density contours (at the $\bar{\Gamma}$ point) in Fig. 6, this SS exhibits typical surface-localized d_{z^2} character. It originates from the bulk nonbonding d_{z^2} state which falls down in energy because of its lowered kinetic energy in the vacuum region. Very recently, Li *et al.*[41] have confirmed the existence of this SS using angle-resolved photoemission. They found that the SS is established for a Gd film as thin as 6–10 Å (two to four monolayers) on the W(110) substrate, indicating the spatial locality of the SS.

The *l*-projected density of states (DOS) in each muffin-tin sphere is plotted in Figs. 7(a) and 7(b) for the FM and AFM cases, respectively. There is a strong similarity between the FM majority and minority-spin DOS curves. Upon comparing them to the DOS curves for the center layer, we see that states at the bottom of the surface *d* bands are shifted markedly to higher energy because of the decreased coordination at the surface. The high peak in the majority-spin surface *d* DOS curve near E_F corresponds to the d_{z^2} SS and other surface resonances. In Fig. 7(b) the more complicated AFM coupling diminishes the similarity between majority- and minority-spin DOS. Nevertheless, the peak of the d_{z^2} SS also exists in the minority-spin surface *d* DOS curve near the Fermi energy.

Note that, as pointed out originally by Freeman and co-workers,[18,19] the band structure of Gd is close to that of hcp transition metals (*d* like), rather than being free-electron-like. In Fig. 5 the 5*d* bands which lie about 1 eV above E_F at the $\bar{\Gamma}$ point are seen to drop sharply below E_F and to hybridize strongly with the *sp* bands, resulting in a flatband dispersion near the edge of the BZ. The calculated total DOS at E_F is quite large, $N(E_F)\approx 1.5$

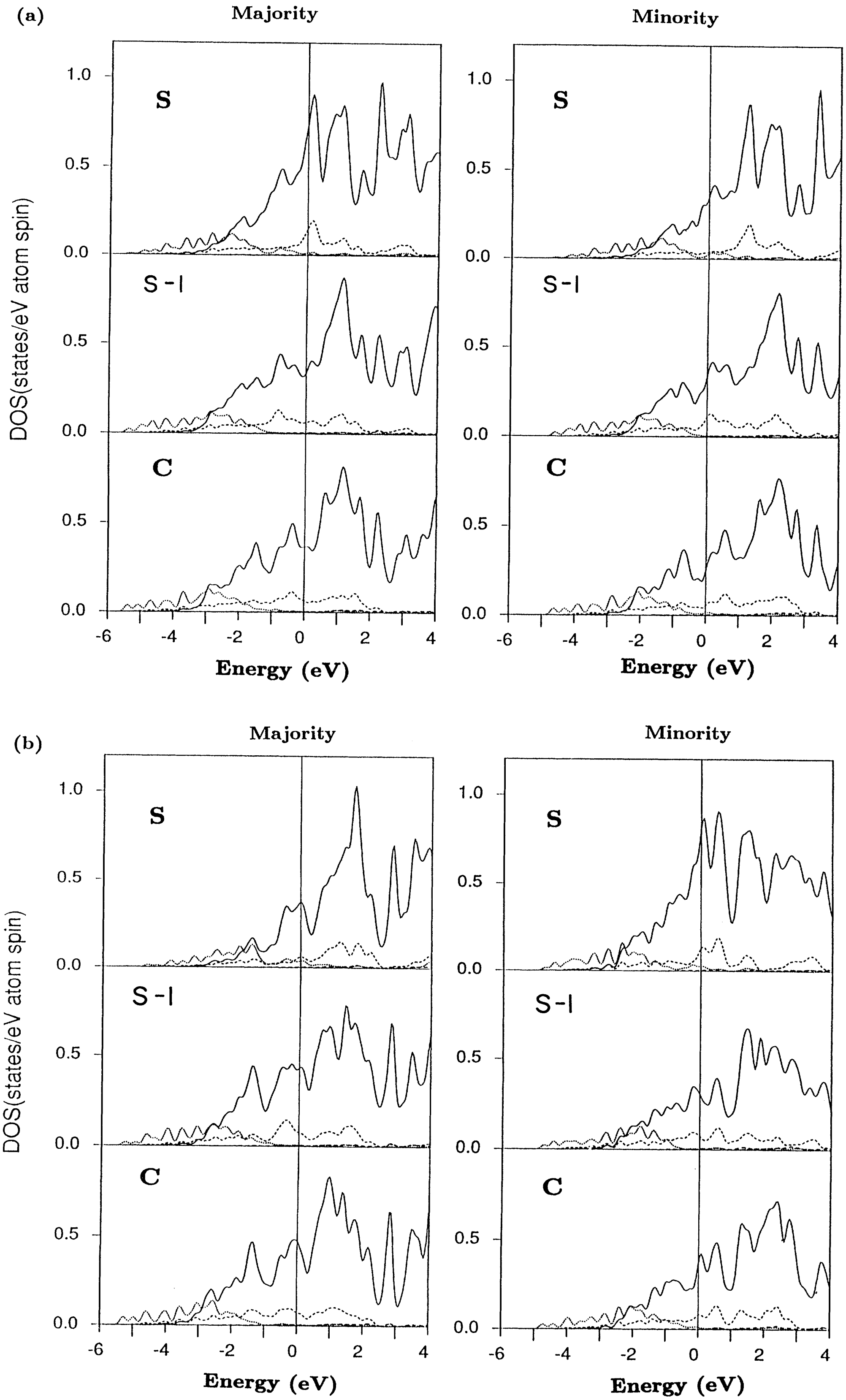

FIG. 7. Angular momentum decomposed density of states projected in muffin-tin spheres for (a) FM Gd(0001) and (b) AFM Gd(0001). Dotted, dashed, and solid lines are for s, p, and d components, respectively.

states/eV per atom. This value agrees fairly well with earlier calculations for hcp and bcc bulk Gd.[19,24,23]

F. Exchange splitting

The average $5d$ band exchange splitting (ΔE_{xc}) is presented in Fig. 8 with respect to the film thickness. For comparison, relevant experimental data obtained from synchrotron radiation photoemission measurements by LaGraffe, Dowben, and Onellion[8] are also given. In general, the theoretical results show the right tendency, but are greater in value than the experimental results. For hcp FM Gd bulk, the theoretical ΔE_{xc} is about 0.85 eV, i.e., 20–25 % higher than the accepted experimental value 0.6–0.7 eV.[42] This discrepancy may be due to the effect of temperature since the theoretical data are for 0 K, but the experimental data were usually taken at a finite temperature.

The ΔE_{xc} for the FM free-standing Gd monolayer is 1.25 eV. As the thickness of the slab increases, ΔE_{xc} converges to about 0.95 eV at the surface layer (solid circles) and to 0.90 eV at the center-layer sites (open circles). For the AFM state, the average exchange splitting of the surface bands is about 1.0 eV. In the few interior layers, the ΔE_{xc} values are considerably lower than for the FM state and converge to the bulk value quite slowly. The calculated ΔE_{xc} at the center layer is 0.62 eV for the six-layer slab, but increases to 0.75 eV for the eight-layer slab.

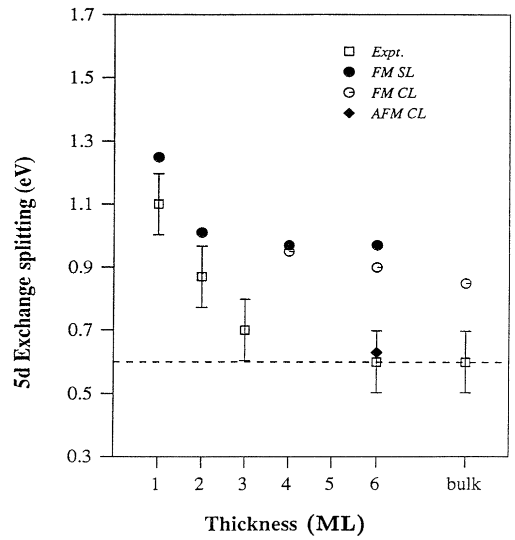

FIG. 8. Exchange splitting of Gd(0001). Solid and open circles represent the theoretical results for the FM Gd(0001) at the surface and center layer, respectively. The rhombus shows the theoretical result at the center layer of a six-layer AFM film. Squares (bars) denote the experimental results obtained by LaGraffe, Dowben, and Onellion (Ref. 8).

IV. SUMMARY AND CONCLUSIONS

The Gd(0001) surface was studied by using the FLAPW total-energy band-structure method. Accurate total-energy results show that the surface Gd atomic layer expands outwardly by 6%. As a result of the enhancement of the second-neighbor interaction between the surface layer and the third layer, the AFM surface coupling becomes more stable than the FM one.

Gd atoms interact via typical metallic bonding since no special bonding orientation exists. Nevertheless, the d band gains in occupation ($1.5e$) more than for the free atom ($1e$), and the DOS in the muffin-tin region is dominated by d character. From the analysis of the electronic and magnetic properties, we found the screening effect to be strong in Gd for both electrostatic and magnetic perturbations (and limited basically to second neighbors).

The existence of the $\bar{\Gamma} d_{z^2}$ surface state is important since it is the origin of the surface magnetic enhancement. The flat dispersion away for the $\bar{\Gamma}$ point suggests that the π interaction between surface atoms is very weak.

ACKNOWLEDGMENTS

Work at Northwestern University was supported by the National Science Foundation (Grant Nos. DMR88-16126 and DMR89-06935) and through a grant of computer time at the Pittsburgh Supercomputing Center from its Division of Advanced Scientific Computing. The work at Oak Ridge National Laboratory was supported by the Division of Materials Science, Office of BES, U.S. Department of Energy under Contract No. DE-AC05-84OR21400 with Martin Marietta Energy System. Inc.

[1]C. Rau and S. Eichner, in *Nuclear Method in Materials Research,* edited by K. Bodge, H. Bauman, H. Jex, and F. Rauch (Vieweg, Braunshweig, 1980), p. 354; C. Rau, J. Magn. Magn. Mater. **31-59**, 874 (1983); C. Rau and S. Eichner, Phys. Rev. B **34**, 6347 (1986); C. Rau and M. Robert, Phys. Rev. Lett. **58**, 2714 (1987).

[2]A. Cerri, D. Mauri, and M. Landolt, Phys. Rev. B **27**, 6526 (1983).

[3]D. Weller, S. F. Alvarado, W. Gudat, K. Schröder, and M. Campagna, Phys. Rev. Lett. **54**, 1555 (1985); D. Weller and S. F. Alvarado, J. Appl. Phys. **59**, 2908 (1986).

[4]D. Weller and S. F. Alvarado, Phys. Rev. B **37**, 9911 (1988).

[5]J. M. Sanchez and J. L. Morán-Lopez, Phys. Rev. Lett. **58**, 1120 (1987).

[6]M. Farle and K. Baberschke, Phys. Rev. Lett. **58**, 511 (1987).

[7]F. J. Himpsel and B. Reihl, Phys. Rev. B **28**, 574 (1983).

[8]D. LaGraffe, P.A. Dowben, and M. Onellion, in *MRS Symposia Proceedings No. 151* (Materials Research Society, Pittsburgh, 1989), p. 71; Phys. Rev. B **40**, 970 (1989).

[9]D. LaGraffe, P. A. Dowben, and M. Onellion, Phys. Rev. B **40**, 3348 (1989).

[10]R. Kammerer, J. Barth, F. Gerken, A. Flodström, and L. I. Johansson, Solid State Commun. **41**, 435 (1982).

[11]J. Kolaczkiewicz and E. Bauer, Surf. Sci. **175**, 487 (1986).

[12]R. M. White, Science **229**, 11 (1985).

[13]B. H. J. Buschow, Rep. Prog. Phys. **40**, 1179 (1977).

[14]M. Taborelli, R. Allenspach, G. Boffa, and M. Landolt, Phys. Rev. Lett. **26**, 2869 (1986); R. Allenspach, M. Taborelli, and M. Landolt, Phys. Rev. B **34**, 6112 (1986).

[15]R. E. Camley, Phys. Rev. B **35**, 3608 (1987).

[16]C. Carbone and E. Kisker, Phys. Rev. B **36**, 1280 (1987).

[17]J. Kwo, E. M. Gyorgy, D. B. McWhan, M. Hong, F. J. DiSalvo, C. Vettier, and J. E. Bower, Phys. Rev. Lett. **55**, 1402 (1985); C. Vettier, D. B. McWhan, E. M. Gyorgy, J. Kwo, B. M. Buntschuh, and B. W. Batterman, *ibid.* **56**, 757 (1986).

[18]J. O. Dimmock, in *Solid State Physics,* edited by H. Ehrenreich, F. Seitz, and D. Turnbull (Academic, New York, 1971), Vol. 64, p. 104; J. J. Rhyne and T. R. McGuire, IEEE Trans. Magn. **8**, 105 (1972); A. J. Freeman, in *Magnetic Properties of Rare Earth Metals,* edited by R. J. Elliott, (Plenum, London, 1972); A. R. Mackintosh, Phys. Today **30 (6)**, 23 (1977).

[19]J. O. Dimmock and A. J. Freeman, Phys. Rev. Lett. **35**, 750 (1964); B. N. Harmon and A. J. Freeman, Phys. Rev. B **10**, 1979 (1974).

[20]P. A. Lindgard, B. N. Harmon, and A. J. Freeman, Phys. Rev. Lett. **35**, 384 (1975).

[21]D. D. Koelling and B. N. Harmon, J. Phys. C **10**, 3107 (1977).

[22]J. Sticht and J. Kübler, Solid State Commun. **53**, 529 (1985).

[23]B. I. Min, H. J. F. Jansen, T. Oguchi, and A. J. Freeman, J. Magn. Magn. Mater. **61**, 139 (1986).

[24]T. C. Leung, X. W. Wang, and B. N. Harmon, Physica B **149**, 131 (1988).

[25]K. Binder and D. P. Landau, Phys. Rev Lett. **52**, 318 (1984); D. P. Landau and K. Binder, Phys. Rev. B **41**, 4633 (1990).

[26]C. Li, A. J. Freeman, and C. L. Fu, J. Magn. Magn. Mater. **83**, 51 (1990).

[27]E. Wimmer, H. Krakauer, M. Weinert, and A. J. Freeman, Phys. Rev. B **24**, 864 (1981), and references cited therein.

[28]U. von Barth and L. Hedin, J. Phys. C **5**, 1629 (1972).

[29]A. J. Freeman and R. Wu, J. Magn. Magn. Mater. (to be published).

[30]C. S. Wang, B. M. Klein, and H. Krakauer, Phys. Rev. Lett. **54**, 1852 (1985).

[31]J. F. Janak and A. R. Williams, Phys. Rev. B **14**, 4199 (1976); K. B. Hathaway, H. J. F. Jansen, and A. J. Freeman, Phys. Rev. B **31**, 7603 (1985).

[32]R. Wu and A. J. Freeman, Phys. Rev. B **44**, 4449 (1991).

[33]See, e.g. *The Structure of Surface II,* edited by J. F. van der Veen and M. A. Van Hove (Springer, New York, 1988); *Proceedings of International Conference on the Structure of Surface III, Milwaukee, 1990,* edited by M. A. Van Hove and S. Y. Tong (Springer-Verlag, Berlin, 1990).

[34]C. Kittel, *Introduction to Solid State Physics,* 5th ed. (Wiley, New York, 1976), p. 85.

[35]We calculated fcc-stacked FM Gd(0001) with $d_{s,s-1}=5.43$ and 5.54 a.u. As the result, the total energy is about 0.8 mRy (same amount as the hcp-stacked case) lower for the latter case. Thereby, relaxations for these two kinds of surface stacking are likely similar.

[36]D. E. Eastman, Phys. Rev. B **2**, 1 (1970).

[37]E. Wimmer, A. J. Freeman, M. Weinert, H. Krakauer, J. R. Hiskes, and A. M. Karo, Phys. Rev. Lett. **48**, 1128 (1982); E. Wimmer, A. J. Freeman, J. R. Hiskes, and A. M. Karo, Phys. Rev. B **28**, 3074 (1983).

[38]L. W. Roeland, G. J. Cock, F. A. Muller, A. C. Moleman, R. G. Jordan, and K. A. McEwen, J. Phys. F **5**, L233 (1975).

[39]C. L. Fu and A. J. Freeman, Phys. Rev. B **35**, 925 (1987); A. J. Freeman, C. L. Fu, M. Weinert, and S. Ohnishi, Hyperfine Interact. **33**, 53 (1987); A. J. Freeman and R. E. Watson, in *Magnetism,* edited by G. T. Rado and H. Suhl (Academic, New York, 1965). Vol. IIA, p. 167.

[40]R. Wu and A. J. Freeman, J. Magn. Magn. Mater. (to be published).

[41]D. Li, C. W. Hutchings, P. A. Dowben, C. Hwang, R. T. Wu, M. Onellion, B. Andrews, and J. L. Erskine, J. Magn. Magn. Mater. (to be published).

[42]A. B. Besnosov, V. V. Eremendo, and V. P. Gnezdilov, J. Magn. Magn. Mater. **43**, 243 (1984); G. Schutz, M. Knulle, R. Wienke, W. Wilhelm, W. Wagner, P. Kienle, and R. Frahm, Z. Phys. B **73**, 67 (1988).